DESIGN OF A MYOELECTRIC CONTROLLER FOR A MULTI-DOF PROSTHETIC HAND BASED ON PRINCIPAL COMPONENT ANALYSIS

Jacob Segil (*Graduate Student, Department of Mechanical Engineering, University of Colorado at Boulder*),
Richard F. *ff*. Weir (*Associate Professor, Department of Bioengineering, University of Colorado at Denver*),
Derek Reamon (*Senior Instructor, Department of Mechanical Engineering, University of Colorado at Boulder*)
1111 Engineering Drive 427 UCB, University of Colorado Boulder, CO 80309-0427

INTRODUCTION

The goal of this investigation is to develop a multi-degree of freedom (DOF) prosthesis controller that uses myoelectric signals as control inputs and which has been dimensionally optimized using Principal Component Analysis (PCA). Currently available multi-DOF hand prostheses cannot be fully utilized because there are fewer control inputs than the number of degrees of freedom (i.e. – joints) that need to be controlled [1]. Based on work from the field of neuroscience [2] it has been shown that grasping is a 'low dimensional' task. Santello et al. used PCA to quantify the principal components (patterns of joint movements) involved in grasping. It was found that grasping tasks involving a number of everyday items could be described by only two principal components. This implies that multi-DOF hand postures can be controlled using only two degrees of control. Therefore, a PCA-based myoelectric prosthetic hand controller can drive grasping postures with only two independent control sites [3],[4]. This is an encouraging finding since current clinical practice indicates two, or three, independent control sites can be located on the residual limb of a typical person with a transradial amputation.

The following paper discusses the design and development of a PCA-based myoelectric prosthetic hand controller. Also, the results of a validation experiment are shared.

METHODS

Design and Development

The design and development of the controller progressed in several distinct steps. The real-time acquisition processing of electromyographic (EMG) signals for two myoelectric sites was developed using standard of care two-site myoelectric control schemes. The PCA algorithm was derived to calculate 15 joint angles of the hand. Several mappings of the EMG signals to the principal component domain were produced. A virtual hand with 15 degree of freedom and anthropomorphic size (50th percentile male) was designed to be controlled in real time. The following sections discuss design and development of the PCA-based myoelectric hand controller in more detail.

Real-time acquisition and processing of two electromyographic (EMG) signals was developed using standard of care to-site myoelectric control schemes. The raw EMG signal was amplified, band passed, rectified and smoothed using typical 2 site myoelectric technique [1].

Following the EMG acquisition and processing, an inverse Principal Component Analysis (PCA) was performed based on work by Santello et al. Santello et al. had subjects grasp 57 household objects while measuring 15 joint angles in the hand. PCA was performed on the empirical data and produced 14 principal component vectors. (The significance of each principal component is determined by the magnitude of the eigenvalue associated with each principal component vector.) Each principal component vector can be considered a 'pattern of movement' between the 15 joints in the hand. This matrix of principal component vectors is used to calculate the 15 joint angles of the hand as described by Equation 1. Each principal component vector ($\vec{[PC]_{,n}}$) is a column vector containing coefficients for each of the 15 joints. The EMG signals are the input to the inverse PCA algorithm and the postural vector made up of 15 joints angles (θ_m) is the output. Notice that this algorithm utilizes the dimensionality reduction properties of PCA by only requiring 2 inputs to control a 15 degree of freedom hand. The 15 degree of freedom hand has been effectively reduced to a two DOF system. The inverse PCA based algorithm and its associated dimensionality reduction differentiates this controller from other multi-function myoelectric prosthesis controllers.

$$\left[\vec{PC_1}\ \vec{PC_2}\ \dots\ \vec{PC_{14}}\right] * \begin{bmatrix} EMG_a \\ EMG_B \\ 0 \\ \dots \\ 0 \end{bmatrix} = \begin{bmatrix} \theta_1 \\ \theta_2 \\ \theta_3 \\ \dots \\ \theta_{15} \end{bmatrix} \qquad (1)$$

As noted above, two EMG signals are used as inputs to the inverse PCA algorithm. However, the EMG signals can be manipulated before the inverse PCA calculation is performed. The EMGs can be mapped on to the principal component domain by the translation and rotation of the axes corresponding to the myoelectric control signals (Figure 1). The solid red axes are the 1st and 2nd principal components which form the PC-domain. The yellow

dashed axes depict a linear orthogonal mapping of the EMG signals to the PC-domain. (The dots are empirical data points from Santello et al.'s grasping trials. The stars are virtual hand postures from this investigation including hand flat (HF), cylindrical prehension (CP), palmar prehension (PP), and lateral prehension (LP).) Notice that the entire PC domain can be described by a linear combination of the EMG signals. This study used both linear orthogonal and non-orthogonal mappings. More complex nonlinear mappings might provide additional benefits and will be studied in the future.

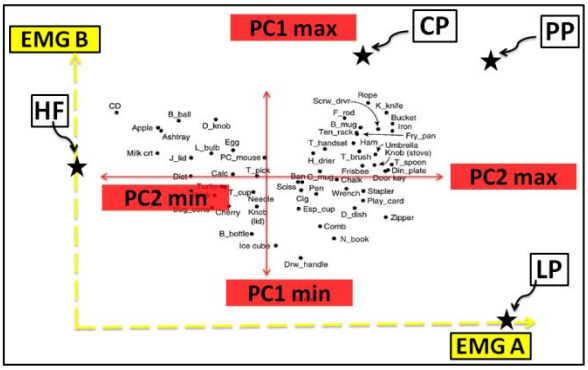

Figure 1: Mapping of EMG signals to PC-domain [2]

The virtual hand design was modeled after the Santello et al. grasping data and built within Labview [5]. The same 15 joints measured by Santello et al. are modeled in the virtual hand (Figure 2). Each digit has two degrees of freedom (the MCP and PIP joints), the thumb has 4 degrees of freedom (the MCP joint, PIP joint, abduction, and rotation), and the middle, ring, and little fingers each have an abduction degree of freedom. The size of the virtual hand and joint axes were modeled after a 50th percentile male hand [6], [7]. A neutral hand posture was derived empirically and is used as the relaxed input to the virtual hand.

Figure 2: Virtual hand model with 15 articulating joints

Validation Experiment

A validation experiment was performed in order to quantify the effectiveness of the PCA based myoelectric controller. Four postures were commanded and the accuracy of the controlled hand compared to the commanded hand was recorded. Also, different mappings of the EMG signals to the principal component domain were tested in order to determine a mapping that is the most functional. The following sections describe the testing procedure in more detail.

The subject population consisted of 5 subjects. The subjects were normal intact individuals who were able to understand and follow directions in English assessed by their ability to respond during the recruitment and consent process. Exclusion criteria included any subjects with trauma to the upper-limbs including amputation and/or are not able to understand the procedures. Informed consent was obtained from all subjects. Standard of care myoelectric control equipment including surface electromyography (EMG) sensors was used to obtain myoelectric signals from the subjects. Standard clinical procedures involving palpation of the subject's arm was used to locate the best positions on the arm for the surface EMG sensors. ProControl2 surface electrodes [8] were placed over the flexor carpi radialis muscle and over the extensor carpi radialis muscles. A forearm sleeve was worn to hold the electrodes in place while water was applied to the control site to aid in the measurement.

The following 4 postures were commanded during the experiment: lateral prehension (LP), palmar prehension (PP), cylindrical prehension (CP), and hand flat (HF). Lateral, palmar, and cylindrical prehension are defined as the most commonly used grasps during activities of daily living while hand flat is typically used as the neutral posture for a prosthetic hand [9]. All 15 joint angles in the hand were used to define the posture.

3 different mappings were tested during the validation experiment. All mappings utilized two site myoelectric control. Map 1 translated the myoelectric signals to the bottom left corner of the principal component domain (Figure 1). Lateral prehension is accomplished moving along the PC1-axis, hand flat is accomplished moving along the PC2-axis, and cylindrical/palmar prehension is accomplished by a strong co-contraction. Map 2 translated and rotated the myoelectric signals to envelop the data points in Santello's principal component domain. Map 2 was tested to investigate whether axes formed by the trending directions of the grasping data from Santello's work had significance. Map 3 used a non-orthogonal axis system. The axis system was defined as having hand flat at the origin, lateral prehension along the first axis, and palmar prehension along the second axis. Cylindrical prehension was accomplished by a slight co-contraction while on the second axis.

The testing sessions began with a thorough description of the testing procedure and the written consent of the subject. A practice session then occurred. During the

practice session, the subject was allowed to control the virtual hand using myoelectric control to gain practice and familiarity with the testing environment. The subject did not use any of the 3 mappings described above during this trial session in order to prevent any familiarity with any of the maps tested. The gain and thresholds of the myoelectric signals were adjusted to provide the most comfortable testing session.

The testing session consisted of 60 randomized trials. Each trial was a combination of a mapping and a posture giving 12 combinations total (ex: Map 1 – Lateral Prehension). Each combination was tested 5 times. The subject was allowed to stop at any point due to fatigue and/or discomfort. The subject was asked to match the image of the controlled hand to the commanded hand within 10 seconds (Figure 3). The subject was provided both the raw EMG signals as well as the joint accuracy measure (an array of lights indicating the percentage of joint accuracy). If the subject achieved the commanded posture, the trial was stopped. At the end of 10 seconds, the trial terminates and the joint accuracy maximum was recorded.

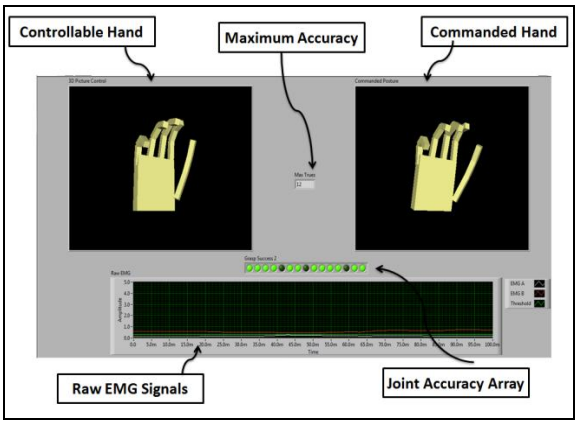

Figure 3: Testing interface

RESULTS

The results of the validation experiment are presented below. A description of the metric studied is followed by the joint accuracy measurements and a description of the statistical methods used. A comparison of the accuracy between postures and between mappings is provided. In conclusion, the favored mapping is found to be more accurate than the other mappings with statistical significance.

Metrics

A maximum joint accuracy percentage was measured during each trial. The joint accuracy metric was defined as the maximum number of joints that are ever simultaneously within the postural envelope. The postural envelope was defined as 25% of the total range of motion of each joint about the target joint angle. This metric is used to compare the accuracy of each posture within each map.

Figure 4 shows the averaged results across all subjects. The accuracy with standard deviation of the four postures is shown for the three maps. It is notable that the accuracy of each posture within any particular mapping is not constant. Also there is a noticeable trend that cylindrical and palmar prehension postures are less accurate than the hand flat and lateral prehension postures across all maps.

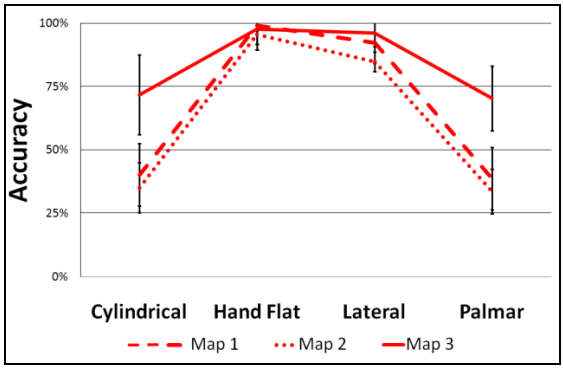

Figure 4: Accuracy of postures across maps

Figure 5 shows the overall accuracy with standard deviation of each mapping across all subjects and postures. Map 3 has a significantly higher accuracy than both Maps 1 and 2.

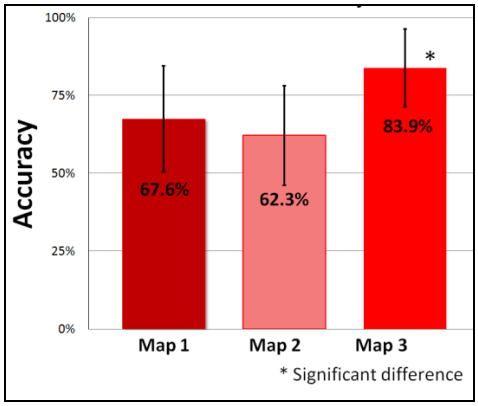

Figure 5: Overall accuracy of maps

In order to verify a significant difference between the accuracy of the three maps an Analysis of Variance (ANOVA) and a Tukey-Kramer test were performed [10]. The null hypothesis for the validation experiment was the following: Map 1, Map 2, and Map 3 produce overall averages that are equal. The validation experiment (300 sample dataset) produced a p-value (2.6E-6) much less than the acceptable type I error (5E-2) and thereby proving the existence of significant differences between the mappings. The Tukey-Kramer test verified that Map 3 is significantly more accurate than Maps 1 and 2.

Discussion

The following sections discuss the trends found from the results of the validation experiment. The functionality of the maps and the correlation between distance from axes and accuracy is analyzed. Also, the rationale behind testing only maps using two control sites and the clinical implications driving the experimental design are reiterated.

Figure 4 depicts several notable trends. Firstly, it is evident that the accuracy of each posture within a particular mapping is not constant. In other words, some postures are more easily achieved than others for each mapping. Specifically, cylindrical and palmar prehensions are the most difficult postures to achieve. This trend suggests a correlation between the ease of achieving the posture and the distance from a posture and an EMG axis. A co-contraction is necessary to move off of a EMG axis. Especially in Maps 1 and 2, the cylindrical and palmar postures are most distant from the EMG signal axes and are also the least accurate postures. In general, it is found that the accuracy measure is dependent upon the amount of co-contraction necessary for each posture.

Figure 4 also shows where Map 3 proves to be more accurate than Maps 1 and 2. The accuracy of cylindrical and palmar prehension when using Map 3 is over 25% greater than when using Maps 1 and 2. All maps achieve the hand flat and lateral prehension postures easily (with accuracy values above 90%).

Figure 5 depicts an overall accuracy (the accuracy of each map across all postures). This further proves the trend seen in Figure 4 that Map 3 is the most accurate and therefore most functional.

It should be reiterated the rationale behind testing various maps using only two control sites. Standard of care procedures today cite two or three surface myoelectric control sites [11] as the most possible after transradial amputation. This fact constricts the design of a myoelectric controller by preventing the use of multiple (greater than two) control signals. Many technologies have been developed to overcome this constraint including hierarchical control schemes and state-machines. However, the dimensionality reduction provided by PCA allows for continuous morphing between postures as opposed to toggling between distinct states. This characteristic is the most significant advancement made by this project.

FUTURE WORK

The myoelectric controller for a multi-DOF prosthetic hand based on principal component analysis developed in this project will be used in future studies. The validation experiment will be further expanded to include more complicated mappings using both nonlinear and non-orthogonal mappings. Also, more control sites (i.e. 3 or 4) will be implemented and tested using more complicated mappings. It is obvious that more control sites will allow for greater ease of use and functionality. Finally, long term questions that stem from this project focus on dexterous manipulation. More specifically, what are the effects of the higher order principal components and how do they relate to dexterous manipulation? The design of a myoelectric controller for a multi-DOF prosthetic hand based on principal component analysis will hopefully act as a foundation for future studies in this pursuit.

ACKNOWLEDGEMENTS

The authors wish to thank their support VA Eastern Colorado Healthcare System - Denver VAMC and the University of Colorado at Boulder Mechanical Engineering Department.

REFERENCES

[1] DS. Childress and RF. *ff* Weir, "Control of Limb Prostheses," in *Atlas of Amputations and Limb Deficiencies: Surgical, Prosthetic, and Rehabilitation Principles*, 3rd ed., 2004, pp. 173-195.

[2] M. Santello, M. Flanders, and JF. Soechting, "Postural hand synergies for tool use," *Journal of Neuroscience*, vol. 18, no. 23, p. 10105, 1998.

[3] G. Magenes, F. Passaglia, and EL. Secco, "A new approach of multi-d.o.f. prosthetic control," pp. 3443-3446, Aug. 2008.

[4] GC. Matrone, C. Cipriani, EL. Secco, G. Magenes, and MC. Carrozza, "Principal components analysis based control of a multi dof underactuated prosthetic hand," *Journal of NeuroEngineering and Rehabilitation*, vol. 7, p. 16, 2010.

[5] National Instruments Inc., "National Instruments Inc.," Austin, Texas. [Online]. Available: http://www.ni.com/. [Accessed: 25-Apr-2011].

[6] AR. Tilley, *The Measure of Man and Woman: Human Factors in Design*. Wiley, 2001.

[7] DARPA, *Revolutionizing Prosthetics Program - Fact Sheet*. 3701 North Fairfax Drive Arlington, VA 22203: Defense Advanced Research Projects Agency, 2008.

[8] Motion Control Inc., "Motion Control Inc.," Salt Lake City, UT. [Online]. Available: http://utaharm.com.

[9] AD. Keller, CL. Taylor, and V. Zahn, *Studies to Determine the Functional Requirements for Hand and Arm Prostheses*. Department of Engineering: University of California at Los Angeles, 1947.

[10] W. Navidi, *Statistics for Engineers and Scientists*, 3rd ed. McGraw-Hill, 2011.

[11] AB. Ajiboye and RF. *ff* Weir, "A heuristic fuzzy logic approach to EMG pattern recognition for multifunctional prosthesis control," *Neural Systems and Rehabilitation Engineering, IEEE Transactions on*, vol. 13, no. 3, pp. 280-291, 2005.